

# Design of Dual-Band Two-Branch-Line Couplers with Arbitrary Coupling Coefficients in Bands

Ivan PRUDYUS, Valeriy OBORZHITSKYI

Institute of Telecommunications, Radioelectronics and Electronic Devices, Lviv Polytechnic National University, St. Bandery st., 12, 79013 Lviv, Ukraine

iprudus@polynet.lviv.ua, oborz@polynet.lviv.ua

**Abstract.** *A new approach to design dual-band two-branch couplers with arbitrary coupling coefficients at two operating frequency bands is proposed in this article. The method is based on the usage of equivalent subcircuits input reactances of the even-mode and odd-mode excitations. The exact design formulas for three options of the dual-band coupler with different location and number of stubs are received. These formulas permit to obtain the different variants for each structure in order to select the physically realizable solution and can be used in broad range of frequency ratio and power division ratio. For verification, three different dual-band couplers, which are operating at 2.4/3.9 GHz with different coupling coefficients (one with 3/6 dB, and 10/3 dB two others) are designed, simulated, fabricated and tested. The measured results are in good agreement with the simulated ones.*

## Keywords

Dual band, branch-line coupler, even-odd-mode excitations, arbitrary coupling coefficient.

## 1. Introduction

Development of the modern wireless communication systems with various frequency standards is accompanied by the active usage of multiband microwave devices. As a directional coupler is one of the base components of Radio Frequency (RF) parts of these systems and can be used in structure of amplifiers, mixers, phase shifters and other devices, therefore in recent years much attention is given to new schemes for the couplers, operating at two arbitrary frequency bands. In the case of widely used branch-line couplers, a lot of dual-band schemes are proposed in the literature. In the majority of reports the structures of relatively simple two-branch-line couplers are considered, two-section topology (tri-branch-line construction) has been used with the object of bandwidth broadening. Among all variety of the offered options of a dual-band two-branch-line coupler realization one can note the next main approaches. It may be the usage of right/left-handed metamaterial transmission lines [1]–[3], the usage

of stretched segments of line [4] or meander lines [5] for branches implementing, the usage of scheme in which all ports are extended through a transmission line section [6]. Very popular approach in obtaining the dual-band operation of the branch-line coupler is based on the use of stub lines. The structures in which open-circuit or short-circuit stubs are connected to all input ports are proposed in [7]. Further similar dual-band structures with some specialized functions were considered in [8]–[12]. In other options of coupler with dual-band response the loading of stub tapped to the center of through lines and branch lines [13]–[16], of branch lines [17], of through lines [18] is used. The difference of structures with stubs consists in a way of stubs realization for achievement of a definite purpose. In [8], for instance, the shunt stubs are folded for placement inside the coupler. The usage of stepped-impedance stubs for compactness and wide range of frequency ratio is proposed in [11], [15]. The multisection stubs, which are employed in [12], allow realizing any required value of shunt input susceptance. The structure, similar to [14] but with the shunt open-circuit dual composite right/left-handed cells, which provide the identical sign of phase difference of output ports within the two operating frequency bands is proposed in [16]. In most cases the principle of equivalent replacement was used for design of dual-band devices. According to this principle it is necessary to do a substitution of each branch of the conventional single-band device by a two-port structure. The  $\pi$ -type or T-type two-ports mostly are used. It is a transmission line segment loaded with shunt susceptance at its ends in the first case [7], [8], [10]–[12], and at its center in the second case [13]–[16]. The electrical parameters (characteristic impedance, electrical length, shunt impedance value) of equivalent structure have to provide the characteristics of removable branch at two frequencies.

Recently, the considerable attention is directed to couplers, which may have arbitrary output power division at the two operation bands. These couplers may be useful at the design of some devices such as antenna arrays, Doherty power amplifiers, mixers and others. In one of the first publications on this subject [8] it is offered to use the equivalent replacement of  $90^\circ$  section with different values of characteristic impedance for different frequencies by a two-port, which consists of a stepped-impedance section

with open stubs attached to its ends. Similar approach but with replacement by conventional  $\pi$ -type two-port with single-section stubs is used in [10], and with multisection stubs in [12]. The other method of obtaining the required output power ratio at the dual frequencies is proposed in [19], [20]. It is based on the replacement of branches by shorted coupled line sections, application of which is obviously connected with certain difficulties because of different even and odd modes phase velocities and the complication of layout.

In this paper, a new method to design dual-band two-branch couplers with the desired coupling coefficients at two operating frequency bands is introduced. As distinct from above mentioned this method is based on the usage of input reactances of two-pole schemes which are obtained by means of the even-mode and odd-mode excitations. At such approach, exact design formulas are received for three options of the dual-band coupler with stub lines, which differ by number and location of stubs. Proposed calculation methods may be used in broad range of frequency ratio and power division ratio. They allow to obtain the different design variants with identical or opposite signs of phase differences within two frequency bands for the selection of variant with physically realizable values of characteristic impedances and shunt susceptances.

## 2. Design Methodology

It is known that the majority of directional couplers have the structure with one or two planes of symmetry. As a rule, for the analysis of a symmetrical four-port network the even-odd-mode decomposition method [21] is used, which is based on the implementation of magnetic and electric walls at this network. In case of bisymmetrical structure we can decompose the network into various single-port subcircuits (even-even, even-odd, odd-even, and odd-odd) by double using the superposition of an even-mode excitation and odd-mode excitation. The corresponding relations between the input resistances of these subcircuits and the scattering parameters of codirectional bisymmetrical coupler at the condition of ideal matching at its ports and ideal isolation are offered in [22]. From these relations it is possible to derive the following expressions for the transmission S-parameters of such lossless coupler:

$$S_{21} = \frac{x_{ee}^2 - x_{oo}^2 + j(x_{ee} - x_{oo} - x_{ee}^2 x_{oo} + x_{ee} x_{oo}^2)}{1 + x_{ee}^2 + x_{oo}^2 + x_{ee}^2 x_{oo}^2}, \quad (1.a)$$

$$S_{31} = \frac{x_{ee}^2 x_{oo}^2 - 1 + j(x_{ee} + x_{oo} + x_{ee}^2 x_{oo} + x_{ee} x_{oo}^2)}{1 + x_{ee}^2 + x_{oo}^2 + x_{ee}^2 x_{oo}^2}. \quad (1.b)$$

In the above,  $S_{21}$  is the transmission coefficient to direct port,  $S_{31}$  is the transmission coefficient to coupled port, and  $x_{ee}$ ,  $x_{oo}$  are the input reactances for the even-even and odd-odd two-pole subcircuits, where the subscripts  $e$  and  $o$  denote the even and odd mode, respectively. The input reactances in (1) are normalized with respect to the refer-

ence (system) impedance  $Z_0$  of the ports. The analysis of equations (1) showed such their peculiarities: 1) a preset combination of values of input reactances gives the required values of S-parameters, and consequently the required distribution of output power; 2) if to reverse the signs of preset values of input reactances, the values of magnitudes of scattering parameters will be not changed but the signs of their phases will be reversed. This also will provide the necessary distribution of output power and the quadrature of phase difference of coupler; 3) if to carry out a mutual exchange of preset values of input reactances, i. e. supply to reactance  $x_{ee}$  the value of reactance  $x_{oo}$ , and the value of reactance  $x_{ee}$  to reactance  $x_{oo}$ , it will provide the required value  $S_{31}$  and will provide the required value of the magnitude of parameter  $S_{21}$  but with a reverse sign of its phase. Such exchange will also give the necessary distribution of output power and the quadrature of phase difference; 4) if to carry out a mutual exchange of preset values of input reactances, as in point 3 but with reverse of their signs it will provide the required value of S-parameters magnitudes but with change of their phase. And such exchange will give the necessary power division ratio and 90 degrees phase difference.

The values of input reactances which provide the necessary value of coupling coefficient  $C$  of a bisymmetrical codirectional lossless coupler at the operating frequency may be calculated as is offered in [22]:

$$x_{ee} = \frac{-1}{x_{oe}} = \frac{|S_{21}| \sin \varphi_{21} + |S_{31}| \sin \varphi_{31}}{1 - |S_{21}| \cos \varphi_{21} - |S_{31}| \cos \varphi_{31}}, \quad (2.a)$$

$$x_{eo} = \frac{-1}{x_{oo}} = \frac{|S_{21}| \sin \varphi_{21} - |S_{31}| \sin \varphi_{31}}{1 - |S_{21}| \cos \varphi_{21} + |S_{31}| \cos \varphi_{31}}, \quad (2.b)$$

$$|S_{21}| = \sqrt{1 - |S_{31}|^2}, \quad |S_{31}| = 10^{-\frac{C}{20}}, \quad \varphi_{21} = \varphi_{31} - \frac{\pi}{2} \quad (2.c)$$

where  $\varphi_{21}$  and  $\varphi_{31}$  are the phases of  $S_{21}$  and  $S_{31}$ , coefficient  $C$  in dB. Unlike other methods, formulas (2) allow at the design of symmetrical directional couplers to preset a value of signal phase on the coupled port and in this way to influence the values of the electrical parameters in the process of their calculation.

### 2.1 Dual-Band Structure with Loaded Ports

Fig. 1(a) shows the structure of branch-line coupler with loaded ports. In [8], [12] for such dual-band structure with arbitrary division of power the calculation method only for  $\varphi_{21} = -\pi$ ,  $\varphi_{31} = -\pi/2$ , was developed on the base of equivalent replacement of  $\lambda/4$  sections. In offered approach by double application of even-odd-mode decomposition the initial structure can be divided into four reduced subcircuits with purely reactive input resistances ( $jX_{ee}$ ,  $jX_{eo}$ ,  $jX_{oe}$ ,  $jX_{oo}$ ) as shown in Fig. 1(b). The normalized input reactances of these reduced circuits can be expressed as follows:

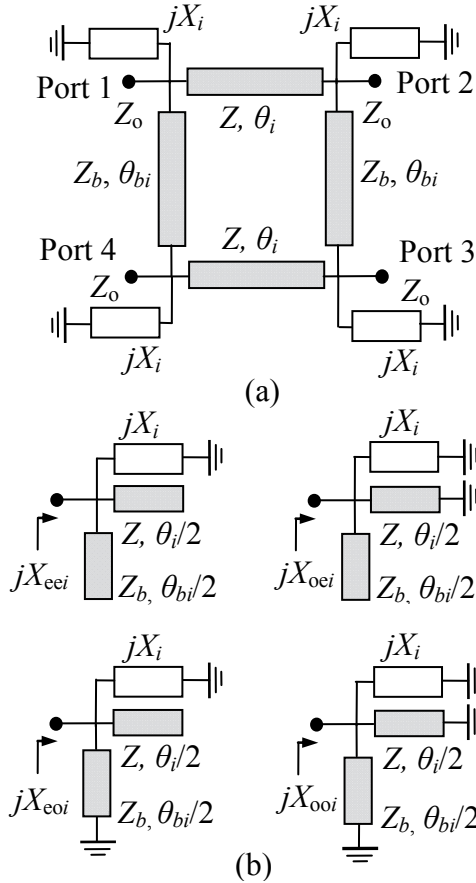


Fig. 1. (a) Dual-band coupler with loaded ports, (b) reduced subcircuits.

$$x_{eei} = \frac{x_i z z_b}{z z_b - x_i (z t_{bi} + z_b t_i)}, \quad (3.a)$$

$$x_{oei} = \frac{x_i z z_b t_{bi}}{z z_b t_{bi} - x_i (z_b t_i t_{bi} - z)}, \quad (3.b)$$

$$x_{oei} = \frac{x_i z z_b t_i}{z z_b t_i - x_i (z t_i t_{bi} - z_b)}, \quad (3.c)$$

$$x_{ooi} = \frac{x_i z z_b t_i t_{bi}}{z z_b t_i t_{bi} + x_i (z t_i + z_b t_{bi})}. \quad (3.d)$$

In (3) subscript  $i = 1, 2$  points to number of frequency, all input reactances, addition reactance  $jX_i$  and characteristic impedances of through lines  $Z$  and branch lines  $Z_b$  are normalized to  $Z_o$ ,  $t_i = \tan(\theta_i/2)$ ,  $t_{bi} = \tan(\theta_{bi}/2)$ , where  $\theta_i$  and  $\theta_{bi}$  are the electrical lengths of lines. It follows from (3), that the functioning of such coupler with different values  $C_i$  at different frequencies can be ensured according to the first stated above feature of the equations (1), if to provide the values of input reactances as required for each frequency. If to use the second feature of the equations (1), when for the search of decision it is necessary to change the signs of input reactances, at that time it is necessary to change the signs of  $X_i$ ,  $t_i$ ,  $t_{bi}$ . The options, which conform to features of the equations (1) with a mutual exchange of the values of input reactances, may be used only to provide

$C_1 = C_2$ . To obtain formulas for calculation of unknown parameters  $Z$ ,  $Z_b$ ,  $X_i$ , we will express  $x_i$  from each of the equations (3), for example:

$$x_i = \frac{x_{eei} z z_b}{z z_b + x_{eei} (z t_{bi} + z_b t_i)}. \quad (4)$$

In the result of equating two pairs of these expressions for  $x_i$ , two formulas for normalized  $Z$  can be derived as

$$z = \frac{-x_{eei}}{x_{eei}^2 + 1} \cdot \frac{t_i^2 + 1}{t_i}, \quad z = \frac{-x_{oei}}{x_{oei}^2 + 1} \cdot \frac{t_i^2 + 1}{t_i}. \quad (5)$$

At the equating of formulas (4) with taking into account the interconnection of input reactances (2), the condition of solution of the set of equations (3) is established:

$$x_{eei} x_{oei} = 1. \quad (6)$$

And the following formula for normalized  $Z_b$  is derived by the equating of two expressions for  $x_i$  with inserting (5) and by the taking into account (6):

$$z_b = \frac{x_{eei}}{x_{eei}^2 - 1} \cdot \frac{t_{bi}^2 + 1}{t_{bi}}. \quad (7)$$

In the result of equating of two expressions which have been written in terms of the first formula (5) for the center frequencies of the lower ( $f_1$ ) and upper ( $f_2$ ) bands (different values of  $i$ ), the following relation is obtained :

$$\frac{x_{ee1}}{x_{ee2}} \cdot \frac{x_{ee2}^2 + 1}{x_{ee1}^2 + 1} = \frac{\sin \theta_1}{\sin(k_f \theta_1)} \quad (8)$$

where  $k_f = f_2/f_1$  is the frequency ratio,  $\theta_1$  and  $\theta_2 = k_f \theta_1$  are the electrical lengths at  $f_1$  and  $f_2$ . At equating of  $z_b$  for different frequencies from (7) the similar relation can be derived as

$$\frac{x_{ee1}}{x_{ee2}} \cdot \frac{x_{ee2}^2 - 1}{x_{ee1}^2 - 1} = \frac{\sin \theta_{b1}}{\sin(k_f \theta_{b1})}. \quad (9)$$

It follows from (2) that the condition (6) can be carried out only when the phase  $\varphi_{31}$  at the coupled output will be equal 0 or  $\pm\pi$ . In this case signals at the outputs will be in a quadrature, if  $\varphi_{21i} = \pm\pi/2$ . Then all input reactances can be expressed by one of them, for example, by  $x_{eei}$ , which depending on a combination of phases  $\varphi_{31}$  and  $\varphi_{21}$  can be determined from (2) as

$$x_{eei} = \pm \sqrt{\frac{1 + |S_{31i}|}{1 - |S_{31i}|}}, \quad x_{eei} = \pm \sqrt{\frac{1 - |S_{31i}|}{1 + |S_{31i}|}} \quad (10)$$

where the first expression is used at  $\varphi_{31i} = 0$  and the second expression is used at  $\varphi_{31i} = \pm\pi$ , the sign before the roots is identical to that for  $\varphi_{21i} = \pm\pi/2$ .

Thus, to define values of all electric parameters of the scheme in Fig. 1(a), it is necessary to set previously values of coupling coefficients and to choose combinations of phases  $\varphi_{31i}$  and  $\varphi_{21i}$  with required signs of phase difference.

By means of (8) and (9) with use of  $x_{cei}$  value calculated by (10) the values of  $\theta_i$  and  $\theta_{bi}$  can be defined. Values of  $X_i$ ,  $Z$ ,  $Z_b$  are calculate by formulas (4), (5) and (7). It should be noted that by a choice of values  $\varphi_{31i}$  and  $\varphi_{21i}$  it is possible to achieve physical realizable values of  $Z$ ,  $Z_b$  and  $X_i$ .

## 2.2 Structure with Four Shunt Reactances

Fig. 2(a) shows the structure of dual-band branch-line coupler with four shunt reactances. Such coupler, but only with the same power division in both bands, was researched in [13]–[16] by using the method of equivalent replacement. In accordance with offered approach as a result of double application of even-odd-mode decomposition method this whole structure can be divided into reduced subcircuits as shown in Fig. 2(b). The normalized input reactances of such subcircuits can be evaluated by the following equations:

$$x_{cei} = \frac{zz_b p_i p_{bi}}{zp_i(z_b - 2x_{bi}t_i) + z_b p_{bi}(z - 2x_i t_i)}, \quad (11.a)$$

$$x_{eoi} = \frac{zz_b p_i t_i}{z_b t_i(z - 2x_i t_i) + zp_i}, \quad (11.b)$$

$$x_{oei} = \frac{zz_b p_{bi} t_i}{zt_i(z_b - 2x_{bi}t_i) + z_b p_{bi}}, \quad (11.c)$$

$$x_{ooi} = zz_b t_i / (z + z_b) \quad (11.d)$$

where  $p_i = 2x_i + zt_i$ ,  $p_{bi} = 2x_{bi} + z_b t_i$ ,  $t_i = \tan(\theta_i/2)$ . For the reduction of quantity of independent variables and also for the simple search of the solution of the electrical length of branch lines in Fig. 2(a) was accepted as equal to length of through sections. If to express  $x_i$ ,  $x_{bi}$ ,  $z_b$  from (11.b), (11.c), (11.d) and to insert these expressions in (11.a), then we reach the previously derived condition of solution (6) of the set of equations (11). Consequently, and for this structure the values of  $x_{cei}$  can be calculated by (10). In the result the expressions for the electrical parameters  $x_i$ ,  $x_{bi}$ , and  $z_b$  can then be expressed in terms of  $x_{cei}$  as follows:

$$x_i = \frac{zt_i[z_b(1 - x_{cei}zt_i) + z]}{2z_b t_i(t_i + x_{cei}z) - z}, \quad (12)$$

$$x_{bi} = \frac{z_b t_i[z_b(1 + x_{cei}zt_i) + z]}{2zt_i(t_i - x_{cei}z_b) - z_b}, \quad (13)$$

$$z_b = -x_{cei}z / (x_{cei} + zt_i). \quad (14)$$

At the equating of  $x_{ooi}$  from formula (11.d) for different frequencies with taking into account that  $x_{ooi} = -x_{cei}$  the following relation is established:

$$\frac{x_{ee1}}{x_{ee2}} = \frac{\tan(\theta_1/2)}{\tan(k_f \theta_1/2)}. \quad (15)$$

Thus, at the beginning of design of coupler with structure in Fig. 2(a) for pre-specified values of  $k_f$ ,  $C_1$ ,  $C_2$

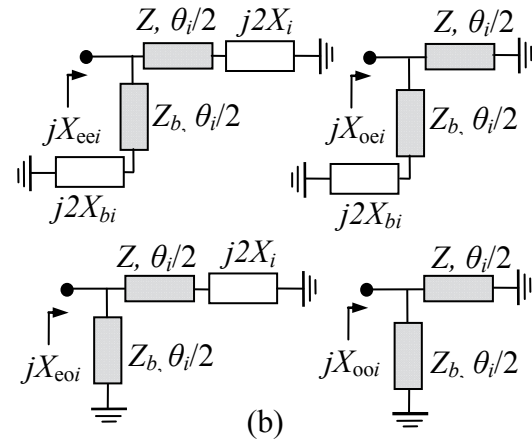
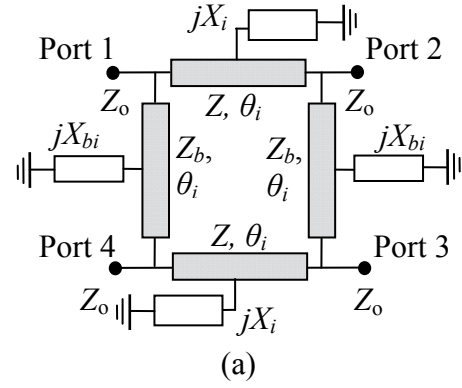


Fig. 2. (a) Structure with four reactances, (b) reduced subcircuits.

and the chosen combination of phases  $\varphi_{31i}$  and  $\varphi_{21i}$  it is necessary to define  $x_{cei}$  by (10),  $\theta_1$  by (15). Further,  $z_b$  is calculated by (14) and the values of  $x_i$ ,  $x_{bi}$  are calculated by (12)–(13) for each frequency. Besides, for computations it is necessary to preset the value of  $Z$  as the number of independent variables exceeds the number of equations. If to assume that  $Z_b = Z$ , then the following formula for  $Z$  can be derived from (14):

$$z = -2x_{cei} / t_i. \quad (16)$$

As in case of the previous structure due to a choice of phases' combinations it is possible as a result of calculation by (12)–(16) to receive different options of electrical parameters and consequently different features of scheme.

## 2.3 Structure with Two Shunt Reactances

Fig. 3 shows the dual-band structures, in which only two additional reactances are used. Such two-branch-line coupler in condition of dual-band operation but only with identical power division is investigated in [17] and [18]. In the first case reactances are attached to the center of branch lines as shown in Fig. 3 (a) and are implemented by open stubs with length equal to  $\theta_i = \theta_{bi}$ . In the second case the through lines of 3-dB coupler are loaded by stubs as in Fig. 3(b) and the length of branch lines is assumed  $\theta_{bi} = 2\theta_i$ .

In the structures under consideration the different length for the through sections and branches is accepted in

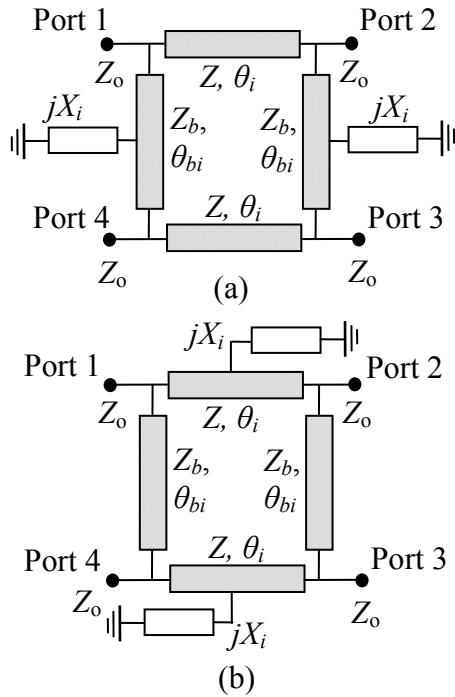


**Fig. 3.** Structures with two reactances, which (a) are attached to branches, (b) are attached to through lines.

order to receive the necessary number of independent variables. If to apply even-odd-mode decomposition twice to structure in Fig. 3(a), then we receive four two-pole subcircuits as in Fig. 2(b) but only without the reactances connected to segments of a through line. For input reactances of these subcircuits the following relations can be written:

$$x_{eei} = \frac{zz_b(2x_i + z_b t_{bi})}{z(z_b - 2x_i t_{bi}) - z_b t_i(2x_i + z_b t_{bi})}, \quad (17.a)$$

$$x_{coi} = zz_b t_{bi} / (z - z_b t_i t_{bi}), \quad (17.b)$$

$$x_{oei} = \frac{zz_b t_i(2x_i + z_b t_{bi})}{z_b(2x_i + z_b t_{bi}) + z t_i(z_b - 2x_i t_{bi})}, \quad (17.c)$$

$$x_{ooi} = zz_b t_i t_{bi} / (z t_i + z_b t_{bi}). \quad (17.d)$$

If to express  $x_i$  from (17.a), (17.c) and  $z$ ,  $z_b$  from (17.b), (17.d) and to equate inter se the expressions for  $x_i$  but with the insertion in these the expressions for  $z$ ,  $z_b$ , then we reach the previously derived condition (6) of solution of the set of equations (17). Taking into account this condition the expressions for  $x_i$ ,  $z$ ,  $z_b$  in terms of  $x_{eei}$  can be written as

$$x_i = \frac{z_b[x_{eei}z - z_b t_{bi}(x_{eei}t_i + z)]}{2[x_{eei}z t_{bi} + z_b(x_{eei}t_i + z)]}, \quad (18)$$

$$z = -\frac{x_{eei}}{x_{eei}^2 + 1} \cdot \frac{t_i^2 + 1}{t_i}, \quad (19)$$

$$z_b = -\frac{x_{eei}}{t_i^2 - x_{eei}^2} \cdot \frac{t_i^2 + 1}{t_{bi}}. \quad (20)$$

In the result of equating of two expressions (19), which have been written for two operation frequencies, the same relation (8) for evaluation of  $\theta_i$  is obtained. In the result of equating of two expressions (20) for two frequencies, the following relation is established:

$$\frac{x_{ee1}}{x_{ee2}} \cdot \frac{t_2^2 - x_{ee2}^2}{t_1^2 - x_{ee1}^2} \cdot \frac{t_1^2 + 1}{t_2^2 + 1} = \frac{\tan(\theta_{bi}/2)}{\tan(k_f \theta_{bi}/2)}. \quad (21)$$

From (21) the values of  $\theta_{bi}$  can be determined for required values of  $x_{eei}$  and  $\theta_i$  value obtained from (8).

For structure in Fig. 3(b) the reduced subcircuits will be as in Fig. 2(b) but only without the reactances connected to segments of a branch line. The input reactances of these subcircuits can be evaluated by the following equations:

$$x_{eei} = \frac{zz_b(2x_i + z t_i)}{z_b(z - 2x_i t_i) - z t_{bi}(2x_i + z t_i)}, \quad (22.a)$$

$$x_{coi} = \frac{zz_b t_{bi}(2x_i + z t_i)}{z(2x_i + z t_i) + z_b t_{bi}(z - 2x_i t_i)}, \quad (22.b)$$

$$x_{oei} = zz_b t_i / (z_b - z t_i t_{bi}). \quad (22.c)$$

Equation for  $x_{ooi}$  is the same as (17.d). By the same procedure as in previous case, from these equations it is possible to receive the following expressions:

$$x_i = \frac{z[x_{eei}z_b - z t_i(x_{eei}t_{bi} + z_b)]}{2[x_{eei}z t_{bi} + z_b(x_{eei}t_i + z)]}, \quad (23)$$

$$z = -\frac{x_{eei}}{t_{bi}^2 + x_{eei}^2} \cdot \frac{t_{bi}^2 + 1}{t_i}. \quad (24)$$

The equation for  $z_b$  is the same as (7), from which the relation (8) is obtained but for  $\theta_{bi}$  determination. If to equate two expressions (24) for different frequencies, we will obtain the relation for  $\theta_i$  determination:

$$\frac{x_{ee1}}{x_{ee2}} \cdot \frac{t_{b2}^2 + x_{ee2}^2}{t_{b1}^2 + x_{ee1}^2} \cdot \frac{t_{b1}^2 + 1}{t_{b2}^2 + 1} = \frac{\tan(\theta_i/2)}{\tan(k_f \theta_i/2)}. \quad (25)$$

In the same way as before at the design of structures in Fig. 3, for pre-specified values of  $k_f$ ,  $C_1$ ,  $C_2$  and the chosen combination of phases  $\varphi_{31i}$  and  $\varphi_{21i}$  it is needed to define  $x_{eei}$  by (10),  $\theta_i$ ,  $\theta_{bi}$  by (8), (21) or by (25), (8) and further to calculate  $Z$ ,  $Z_b$  by (19), (20) or by (24), (7) and  $X_i$  values by (18) or by (23) for two frequencies. The results of calculations depend on a combination of  $\varphi_{31i}$ ,  $\varphi_{21i}$ .

## 2.4 Realization of Dual-Frequency Reactances

Dual-band operation of above-mentioned structures requires the usage of additional reactances. For their realization it is possible to use both open or short circuit transmission line stubs and different types of multisection stubs formed by transmission line segments connections. Fig. 4 shows some options of such circuits. Their input reactances

at frequencies  $f_1$  and  $f_2$  have to be respectively equal to  $X_1$  and  $X_2$  values. It can be provided by means of two independent electrical parameters (of two independent variables). The application with this purpose of an open-circuit stub or a short-circuit stub is a simplest. In this case their  $\theta_1$  electrical length can be defined from (15) where instead of the relation  $x_{ee1}/x_{ee2}$  it is necessary to use  $X_2/X_1$  relation for the opened stub or  $X_1/X_2$  for the shorted stub. Application of such stubs is limited to admissible  $X_i$  values and in many cases gives physically unrealizable results therefore more complex structure can be used.

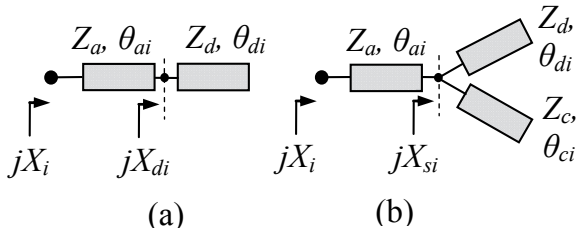


Fig. 4. (a) Stepped-impedance stub, (b) multisection stub.

The stepped-impedance-stub line in Fig. 4(a) is the series connection of two transmission line segments with different characteristic impedances  $Z_a$ ,  $Z_d$  and electrical length  $\theta_{ai}$ ,  $\theta_{di}$ . Opened or shorted at the end second segment must provide such  $X_{di}$  values of the input reactances, which can be transformed by the first segment to demanded  $X_i$  values. In this case there is a surplus of independent parameters therefore search of the solution can be carried out by various ways depending on basic data. For example, if  $Z_a$  of the first segment and its electrical length  $\theta_{a1}$  (consequently  $\theta_{a2} = k_f \theta_{a1}$ ) are given, the  $X_{di}$  can be defined as

$$X_{di} = Z_a (X_i - Z_a \cdot t_{ai}) / (Z_a + X_i t_{ai}) \quad (26)$$

where  $t_{ai} = \tan(\theta_{ai})$ , parameters  $Z_a$ ,  $X_i$ ,  $X_{di}$  are unrationed. Further, by method of calculation of single stub the electrical parameters of the second segment can be defined for the  $X_{di}$  values derived from (26). With a choice of other pair of independent variables the solution can be derived by iterative search of roots of the transcendental equations. Structure in Fig. 4(b) is formed by the connection of transmission line segment with a T-junction or Y-junction of transmission lines or with a segment of coupled lines. For the electrical parameters of this circuit the following relation is established:

$$(1/X_{di} + 1/X_{ci})(X_i - Z_a t_{ai})Z_a = Z_a + X_i t_{ai} \quad (27)$$

where  $X_{di}$ ,  $X_{ci}$  are the input reactances of segments with characteristic impedances  $Z_d$ ,  $Z_c$  and electrical length  $\theta_{di}$ ,  $\theta_{ci}$ . Whereas only two independent variables must be then values of four parameters need to be set, and so the calculations can be carried out by different ways. If to set, for example,  $Z_a$ ,  $\theta_{a1}$  provided that  $Z_d = Z_c$ ,  $\theta_{di} = \theta_{ci}$ , then an input reactance  $X_{di}$  of each branch will be twice more than value calculated by (26). In this case instead of Y-junction it is possible to use a segment of coupled lines

with joining of pair of its ends to the first segment. Thanks to even-mode excitation of coupled lines the characteristic impedance  $Z_c$  of even mode must be equal to  $Z_d$ , and the electrical length  $\theta_{ei}$  of even mode must be equal to  $\theta_{di}$ . At the same time the parameters of odd-mode excitation don't influence scheme characteristics. The values of  $Z_d$ ,  $\theta_{di}$  or  $Z_c$ ,  $\theta_{ei}$  can be determined from  $X_{di}$  values in way of the single stub. At other option of Fig. 4(b) structure calculation the values of  $Z_a$ ,  $Z_d$  and  $\theta_{ai}$ ,  $\theta_{di}$  can be preset. The  $X_{ci}$  values, which are necessary for definition  $Z_c$ ,  $\theta_{ci}$  can be calculated by (27). In accordance with approach which was considered in [12] one branch-line of Fig. 4(b) is assumed to be a quarter-wavelength long at one of the operating frequencies, and values of  $Z_a$ ,  $Z_d$ ,  $Z_c$  are preset. If, for example,  $\theta_{c1} = 90^\circ$ , then  $X_{c1} = 0$  (if the opened end) and therefore  $t_{a1} = X_1/Z_a$ . Further, from (27) for known  $Z_a$ ,  $t_{a2}$ ,  $X_{c2}$ ,  $X_{d2}$  can be defined, and then  $Z_c$  and  $\theta_{ci}$  can be calculated. The other options of a choice of unknown parameters lead to the transcendental equations. Due to possibility of deriving the different results depending on initial data and consequently of deriving a different frequency dependence of  $jX$  in operating bands for structures in Fig. 4, thereby it is possible to influence characteristics of a branch-line coupler.

### 3. Simulated and Measured Results

To verify the offered design concept, and also for study of structures features, borders of their possible application each variant of a coupler was in detail investigated by calculations and simulation. In order to take into the account the effect of junction discontinuities and open-end effect, the tuning of layouts were carried out by using an electromagnetic solver. For experimental demonstration, the dual-band couplers were fabricated using the microstrip transmission lines on a Teflon substrate with dielectric constant of 2.68 and a thickness of 1.45 mm. Electrical parameters of these couplers, which are denominated further as A, B, C and values of geometrical sizes appropriate to them, which are received after correction by means of electromagnetic simulation, are listed in Tab. 1.

*A. Coupler with loaded ports.* Results of calculations of such a coupler by means of expressions given in Sec. 2.1, completely coincide with the results [8] (4.76/6.97 dB at 2.45/5.2 GHz), [12] (3/1.76 dB at 1.96/3.5 GHz), which are obtained only for one combination of phases  $\varphi_{31i} = -\pi$ ,  $\varphi_{21i} = -\pi/2$  at two frequencies.

The offered method allows designing the devices with smaller value of  $k_f$  thanks to possibility of a choice of different combinations of phase  $\varphi_{31i}$ ,  $\varphi_{21i}$  at the operating frequencies. Tab. 2 gives the comparison of minimum values of frequency ratio  $k_f$ , which are permissible from point of view of the realizable values of characteristic impedances at various values of  $C_1$  and various ratios  $C_1$  to  $C_2$  for proposed method at  $\varphi_{31i} = -\pi$ ,  $\varphi_{211} = -\pi/2$ ,  $\varphi_{212} = \pi/2$ , for example, and methods [8], [12].

Coupl.	Z (Ω)	W (mm)	θ <sub>1</sub> °	l (mm)	Z <sub>b</sub> (Ω)	W (mm)	θ <sub>b1</sub> °	l (mm)	X <sub>i</sub> (Ω)	X <sub>bi</sub> (Ω)
A	58.6	2.8	143	35.2	100.5	1.0	150.2	32.0	58.6/-46.5	-
B	54	3.4	129.4	30.4	83.3	1.8	-	-	416.1/-338.2	-26.5/-70.3
C	65.5	2.4	133.6	28.2	60.25	2.8	129.3	31.8	-15.1/45.35	-

Tab. 1. Circuit parameters and geometrical sizes of the three experimental couplers.

C <sub>1</sub> (dB)	1.5		3		6		10	
C <sub>1</sub> /C <sub>2</sub>	[8]	Prop.	[8]	Prop.	[8]	Prop.	[8]	Prop.
0.3	2.1	1.2	-	1.4	-	-	-	-
0.4	1.8	1.15	2.2	1.2	-	1.7	-	-
0.6	1.3	1.1	1.5	1.1	1.9	1.35	2.3	2
0.8	1.1	-	1.1	-	1.3	1.3	1.4	1.6

Tab. 2. Permissible values of k<sub>f</sub> for the coupler A with loaded ports.

The coupler of this kind for the coupling coefficients 3/6 dB at 2.45/3.9 GHz (k<sub>f</sub>= 1.59, inadmissible value for methods [8], [12]) has been designed by the proposed method and then fabricated and measured. Influence of various combinations of phases upon the values of electrical parameters is evident from the results given for this coupler in Tab. 3. This affect can be used for choice of variant with smaller sizes (shorter segments) or with characteristic impedances, which are possible to implement.

φ <sub>311</sub>	φ <sub>312</sub>	φ <sub>211</sub>	φ <sub>212</sub>	Z (Ω)	θ <sub>1</sub> °	Z <sub>b</sub> (Ω)	θ <sub>b1</sub> °
0	0	-π/2	-π/2	43.3	54.6	136.3	201.5
0	π	π/2	π/2	81	205.9	100.5	150.2
0	π	-π/2	π/2	58.6	143	136.1	201.5
-π	0	-π/2	-π/2	43.3	56.4	100.5	150.2
-π	-π	π/2	π/2	81	205.9	136.3	201.5
-π	-π	-π/2	π/2	58.6	143	100.5	150.2

Tab. 3. Dependence of electric parameters of the coupler with loaded ports A from combinations of phases.

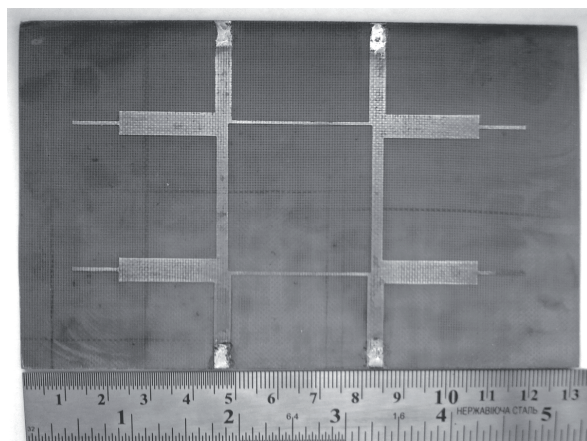


Fig. 5. Photograph of fabricated coupler A with loaded ports.

In Tab. 1, the values of electrical parameters of coupler A are given, which are calculated by using (4)-(10) for chosen combination of phases φ<sub>311</sub>= -π, φ<sub>211</sub>= -π/2, φ<sub>212</sub>= +π/2 and its sizes. Reactances of X<sub>i</sub> were realized by structure as in Fig. 4(a) with electrical parameters

Z<sub>a</sub>= 38.2 Ω, Z<sub>d</sub>= 102.7 Ω, θ<sub>a1</sub>= 100°, θ<sub>d1</sub>= 49° calculated by using (26). Fig. 5 shows the photograph of the fabricated dual-band coupler. Fig. 6 shows the simulated and measured scattering parameters of the coupler. The measured results indicate that the dual-band operation for small k<sub>f</sub> has been achieved with a slight deviation of a coupling level at center frequencies from desired values. The insertion loss are |S<sub>21</sub>| = -3.12 dB and |S<sub>31</sub>| = -3.45 dB at 2.45 GHz and |S<sub>21</sub>| = -1.61 dB and |S<sub>31</sub>| = -6.73 dB at 3.9 GHz, respectively. The opposite sign of a phase difference φ<sub>21i</sub> - φ<sub>31i</sub> at f<sub>1</sub> and f<sub>2</sub> is caused by the choice at calculations of an opposite sign of φ<sub>21i</sub> at these frequencies. Information on bandwidths of this coupler A is given in Tab. 4.

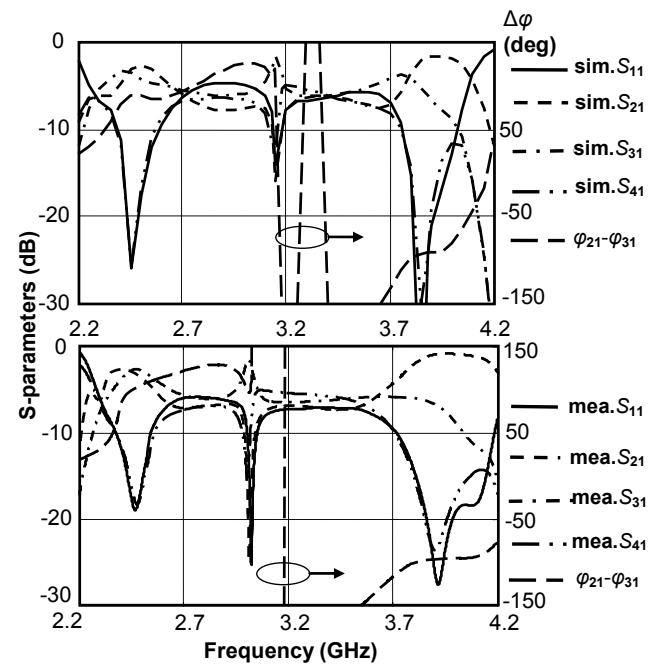


Fig. 6. Simulated and measured S-parameters of coupler A with loaded ports.

Coupler		1/ S <sub>11</sub>   (>15 dB)	1/ S <sub>41</sub>   (>15 dB)	φ <sub>21</sub> - φ <sub>31</sub> (±90°±5°)
	A	Sim.	4.0/4.4	4.0/3.6
	Meas.	3.9/8.2	3.9/5.6	5.0/8.1
B	Sim.	-3.6	-3.6	11.6/3.4
	Meas.	8.4/3.0	-5.3	10.0/3.7
C	Sim.	-3.6	-3.4	11.1/3.4
	Meas.	11.8/3.0	-3.9	11.5/3.8

Tab. 4. Bandwidths % of the three experimental dual-band couplers.

**B. Coupler with four shunt reactances.** Results of calculations of such coupler by an offered method coincide with the results [13] (0.9/2 GHz), [15] (2.4/5.8 GHz), which are obtained only for  $C_1 = C_2$  at one combination of phases  $\varphi_{31i} = -\pi$ ,  $\varphi_{211} = -\pi/2$ ,  $\varphi_{212} = +\pi/2$ .

The identical signs of a phase difference at  $f_1$  and  $f_2$  of this structure with different power division can be achieved at short segments of lines only for ratio  $C_1/C_2 = 0.2-0.8$ ,  $k_f < 1.8$  and only at long segments for greater values of this ratio and  $k_f$ . The possibility to receive the values of impedances which are admissible for realization depends from the choice of phases combination and of  $Z$  value. Tab. 5 gives the examples of calculation of coupler parameters, which can serve as corroboration of the told.

$\varphi_{311}/\varphi_{312}$ $\varphi_{211}/\varphi_{212}$	$C_1/C_2$ (dB)	$k_f$	$\theta_1^\circ$	$Z$ ( $\Omega$ )	$Z_b$ ( $\Omega$ )
$-\pi/-\pi$ $-\frac{\pi}{2}/-\frac{\pi}{2}$	3/6	1.2	92.8	50	32.5
				30	57.3
$-\frac{\pi}{2}/-\frac{\pi}{2}$	3/7.5	1.4	57.9	50	148
				100	59.7
$0/\pi$ $-\frac{\pi}{2}/\frac{\pi}{2}$	3/1	1.8	162.9	30	46.1
				50	28.6
$-\frac{\pi}{2}/\frac{\pi}{2}$	6/3	2.4	128.2	50	267.2
				100	72.8
$0/0$	6/3	2.4	245.7	100	127.3
$\frac{\pi}{2}/\frac{\pi}{2}$				150	89.4

**Tab. 5.** Parameters of coupler with four shunt reactances B at the identical signs of phase difference.

The coupler with this structure can be used for dual-band work with a considerable difference of coupling coefficients  $C_i$ . This is demonstrated by the following example. The coupler for the coupling coefficients 10/3 dB at 2.4/3.9 GHz has been designed by the proposed method then has been fabricated and measured. The electrical parameters of this coupler B, which are calculated by using (12)-(15) for phases  $\varphi_{31i} = 0$ ,  $\varphi_{211} = -\pi/2$ ,  $\varphi_{212} = +\pi/2$  and its

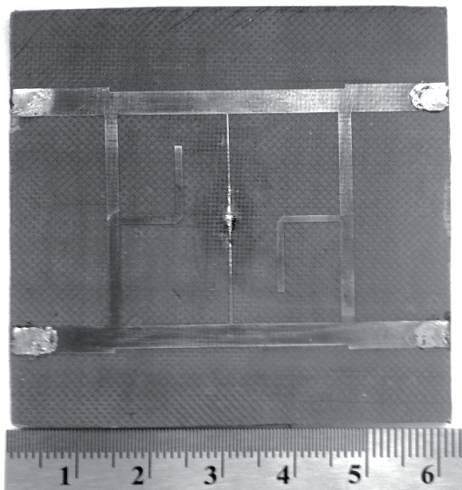


**Fig. 7.** Photograph of fabricated coupler B with four shunts.

sizes are given in Tab. 1. Reactances of  $X_i$  were realized by the short-circuit stub with electrical parameters  $Z = 150.61 \Omega$ ,  $\theta_1 = 70.1^\circ$ , and reactances of  $X_{bi}$  were realized by the open-circuit stub with parameters  $Z = 106.17 \Omega$ ,  $\theta_1 = 76^\circ$ . Fig. 7 shows the photograph of the fabricated coupler, and Fig. 8 shows the simulated and measured frequency responses of it, which agree closely with each other.

The measured data reveal that the required values of the insertion losses of a coupled port are obtained at 2.46/3.97 GHz with the phase differences of  $95^\circ/+86^\circ$ . The small discrepancies between the simulated and measured results can be explained by deviation of a dielectric constant of substrate from a value used at calculations and by the limited accuracy of the prototypes fabrication. Tab. 4 gives the values of coupler B bandwidths.

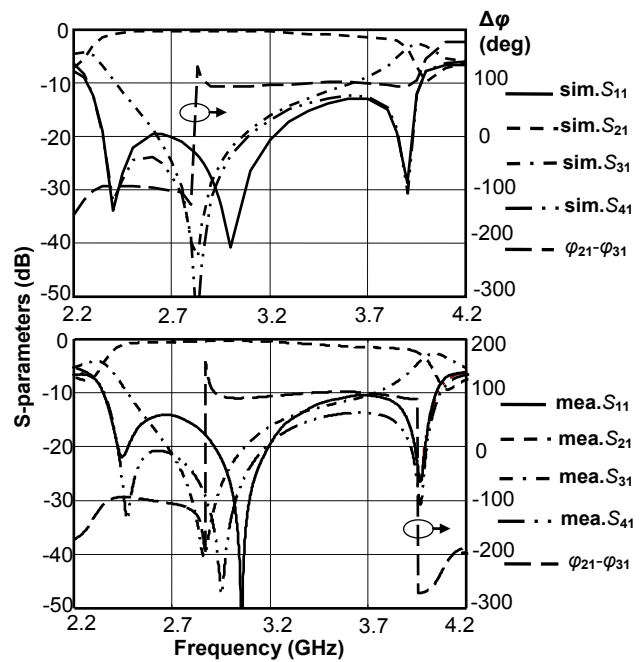


**Fig. 8.** Simulated and measured S-parameters of coupler B with four shunts.

**C. Coupler with two shunt reactances.** The calculations of such couplers showed that for structure in Fig. 3(b), physically admissible values of characteristic impedances issue for  $k_f > 1.8$  and at different signs of  $\varphi_{21i}$ . The structure as in Fig. 3(a) gives more capabilities for use. Results of calculations of such coupler with  $C_i = 3$  dB at 1/2.4 GHz and  $\varphi_{31i} = \pi$ ,  $\varphi_{211} = -\pi/2$ ,  $\varphi_{212} = \pi/2$  by the offered method completely coincide with results of method [17], which was developed for  $C_1 = C_2$  and opposite signs of phase difference at  $f_1$  and  $f_2$ . The identical signs may be achieved by the proposed method in broad range of  $k_f$  thanks to selection of combination  $\varphi_{31i}$ ,  $\varphi_{21i}$ . Tab. 6 gives the results, which corroborate that.

Results, acceptable for realization with the opposite signs of a phase difference may be obtained both at small difference of coupling coefficients and like the previous case at a big difference of them, which can be illustrated by



$C_1/C_2$ (dB)	$\varphi_{311}/\varphi_{312}$ $\varphi_{211}/\varphi_{212}$	$k_f$	$\theta_1^\circ$	$Z$ ( $\Omega$ )	$\theta_{b1}^\circ$	$Z_b$ ( $\Omega$ )
3/6	$0/\pi$ $-\frac{\pi}{2}/\frac{\pi}{2}$	1.5	147.5	65.7	168.7	25.8
		1.7	138.2	52.9	172.7	66.3
	$\pi/\pi$ $-\frac{\pi}{2}/\frac{\pi}{2}$	1.8	134.2	49.3	99.2	21.4
		2.2	126.0	43.7	35.4	85.4
6/3	$0/\pi$ $-\frac{\pi}{2}/\frac{\pi}{2}$	1.6	134.6	60.8	168.0	22.6
		1.8	123.8	52.1	172.3	52.8
	$0/0$ $-\frac{\pi}{2}/-\frac{\pi}{2}$	1.9	68.7	46.4	291.4	73.4
		2.1	63.4	48.4	258.5	37.3
	$\pi/\pi$ $-\frac{\pi}{2}/-\frac{\pi}{2}$	2.2	61.0	49.5	175.2	111.9
		2.4	57.0	51.6	183.4	29.3

Tab. 6. Parameters of coupler C with two shunt reactances at the identical signs of phase difference.

the following example. Calculation of coupler C with the same values 10/3 dB of coupling coefficients at frequencies 2.45/3.9 GHz for the same combination of phases  $\varphi_{31i} = 0$ ,  $\varphi_{211} = -\pi/2$ ,  $\varphi_{212} = +\pi/2$  by means of (18)-(21) gave the values of electrical parameters, which are listed together with sizes in Tab. 1. Reactances of  $X_i$  were realized by the open-circuit stubs with parameters  $Z = 68.45 \Omega$ ,  $\theta_1 = 77.58^\circ$ . Fig. 9 shows the photograph of dual-band coupler fabricated by sizes, specified as a result of electromagnetic simulation. Fig. 10 shows the simulated and measured coupler frequency responses which are very similar to the previous case. Required values of coupling coefficients are obtained at frequencies of 2.47/3.96 GHz with the phase differences of  $95^\circ/89^\circ$ . Discrepancies between the simulated and measured results are caused by the same as stated above. The values of coupler bandwidths are given in Tab. 4. This type of a dual-band coupler is simpler in fabrication, has smaller quantity of discontinuities and the smaller sizes.

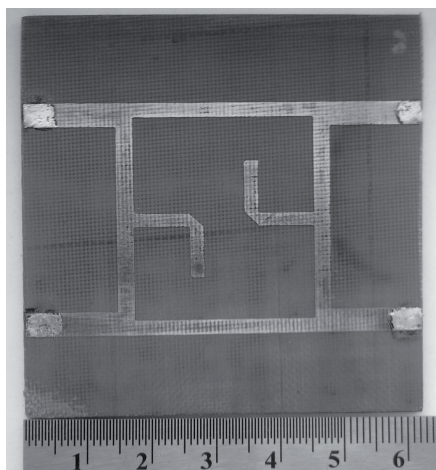


Fig. 9. Photograph of fabricated coupler C with two shunts.

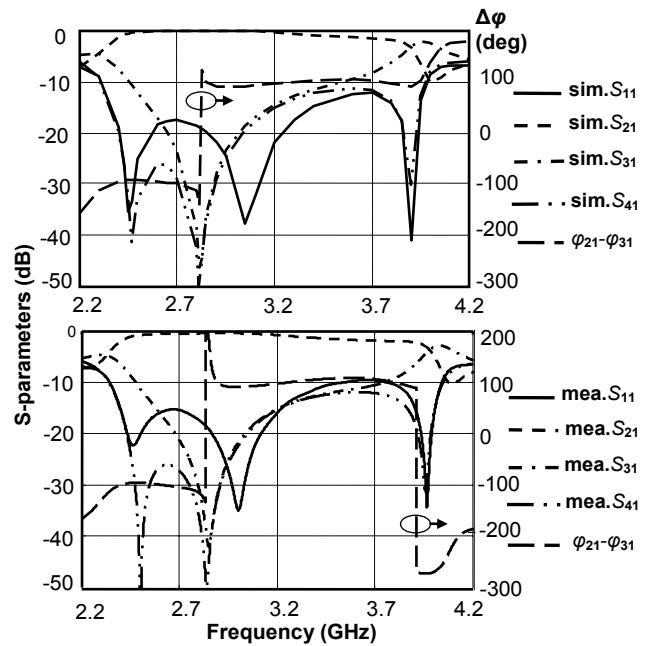


Fig. 10. Simulated and measured S-parameters of coupler C with two shunts.

### 4. Conclusions

The new approach to the design of dual-band two-branch-line directional couplers with arbitrary coupling coefficient at operating frequencies offered in this paper is based on the use of networks input impedances, which are obtained by even-odd-mode excitations. Three options of couplers with bisymmetrical structures, which contain four or two addition reactances are considered. Closed-form design equations have been formulated for the evaluation of parameters of their circuits. The proposed methods of calculation gives more design flexibility of coupler because of the possibility of choice of a suitable phases combination on outputs. For verification, three experimental dual-band circuits operating at 2.45/3.9 GHz with different coupling coefficients are demonstrated. Good agreement between the simulated and measured results has been observed. The proposed approach may easily be extended to the design of other directional couplers with two symmetry planes.

### Acknowledgements

The authors would like to thank Prof. Yevhen Yashchyshyn and the research workers of the Institute of Radioelectronics, Warsaw University of Technology for their help in experimental investigations.

### References

[1] LIN, X. Q., LUI, R. P., YANG, X. M., CHEN, J. X., YIN, X. X., CHENG, Q., CUI, T. J. Arbitrary dual-band components using

- simplified structures of conventional CRLH TLs. *IEEE Transactions on Microwave Theory and Techniques*, 2006, vol. 54, no. 7, p. 2902–2909.
- [2] CHI, I.-H., DeVINCENTIS, M., CALOZ, C., ITOH, T. Arbitrary dual-band components using composite right/left-handed transmission lines. *IEEE Transactions on Microwave Theory and Techniques*, 2004, vol. 52, no. 4, p. 1142–1149.
- [3] LIN, P.-L., ITOH, T. Miniaturized dual-band directional couplers using composite right/left-handed transmission structures and their applications in beam pattern diversity systems. *IEEE Transactions on Microwave Theory and Techniques*, 2009, vol. 57, no. 5, p. 1207–1215.
- [4] WONG, F.-L., CHENG, K.-K. M. A novel planar branch-line coupler design for dual-band applications. In *IEEE MTT-S Int. Microwave Symp. Dig.*, 2004, vol. 2, p. 903–906.
- [5] JIZAT, N. M., RAHIM, S. K. A., RAHMAN, T. A., ABDULRAHMAN, A. Y., SABRAN, M. I., HALL, P. S. Miniaturized size of dual-band-meandered branch-line coupler for WLAN application. *Microwave and Optical Technology Letters*, 2011, vol. 53, no. 11, p. 2543–2547.
- [6] KIM, H., LEE, B., PARK, M.-J. Dual-band branch-line coupler with port extensions. *IEEE Transactions on Microwave Theory and Techniques*, 2010, vol. 58, no. 3, p. 651–655.
- [7] CHENG, K.-K., M., WONG, F.-L. A novel approach to the design and implementation of dual-band compact planar 90° branch-line coupler. *IEEE Transactions on Microwave Theory and Techniques*, 2004, vol. 52, no. 11, p. 2458–2463.
- [8] HSU, C.-L., M., KUO, J.-T., CHANG, C.-W. Miniaturized dual-band hybrid couplers with arbitrary power division ratios. *IEEE Transactions on Microwave Theory and Techniques*, 2009, vol. 57, no. 1, p. 149–156.
- [9] TANG, C.-W., CHEN, M.-G. Design of multipassband microstrip branch-line couplers with open stubs. *IEEE Transactions on Microwave Theory and Techniques*, 2009, vol. 57, no. 1, p. 196–203.
- [10] KIM, K., LIM, J., KIM, K., AHN, D. A compact dual band branch line coupler with arbitrary power division ratio. *Microwave and Optical Technology Letters*, 2010, vol. 52, no. 7, p. 1476–1480.
- [11] ZHENGL, N., ZHOU, L., YIN, W.-Y. A novel dual-band  $\Pi$ -shaped branch-line coupler with stepped-impedance stubs. *Progress In Electromagnetics Research Letters*, 2011, vol. 25, p. 11–20.
- [12] RAWAT, K., RAWAT, M., HASHMI, M. S., GHANNOUCHI, F. M. Dual-band branch-line hybrid with distinct power division ratio over the two bands. *International Journal of RF and Microwave Computer-Aided Engineering*, 2013, vol. 23, no. 1, p. 90–98.
- [13] ZHANG, H., CHEN, K. J. A stub tapped branch-line coupler for dual-band operations. *IEEE Microwave and Wireless Components Letters*, 2007, vol. 17, no. 2, p. 106–108.
- [14] PARK, M.-J. Dual-band, unequal length branch-line coupler with center-tapped stubs. *IEEE Microwave and Wireless Components Letters*, 2009, vol. 19, no. 10, p. 617–619.
- [15] CHIN, K.-S., LIN, K.-M., WEI, Y.-H., TSENG, T.-H., YANG, Y.-J. Compact dual-band branch-line and rat-race couplers with stepped-impedance-stub lines. *IEEE Transactions on Microwave Theory and Techniques*, 2010, vol. 58, no. 5, p. 1213–1221.
- [16] LU, K., WANG, G.-M., TIAN, B. Design of dual-band branch-line coupler based on shunt open-circuit DCRLH cell. *Radioengineering*, 2013, vol. 22, no. 2, p. 618–623.
- [17] KIM, T. G., LEE, B., PARK, M.-J. Dual-band branch-line coupler with two center-tapped stubs. *Microwave and Optical Technology Letters*, 2008, vol. 50, no. 12, p. 3136–3139.
- [18] JIZAT, N. M., RAHIM, S. K. A., RAHMAN, T. A., KAMARUDIN, M. R. Miniaturize size of dual band branch-line coupler by implementing reduced series arm of coupler with stub loaded. *Microwave and Optical Technology Letters*, 2011, vol. 53, no. 4, p. 819–822.
- [19] HSU, C.-L. Dual-band branch line coupler with large power division ratios. In *Proceedings of Asia Pacific Microwave Conference*. Singapore, 7-10 Dec. 2009, p. 2088–2091.
- [20] YU, C.-H., PANG, Y.-H. Dual-band unequal-power quadrature branch-line coupler with coupled lines. *IEEE Microwave and Wireless Components Letters*, 2013, vol. 23, no. 1, p. 10–12.
- [21] REED, J., WHEELER, G. J. A method of analysis of symmetrical four-port networks. *IEEE Transactions on Microwave Theory and Techniques*, 1956, vol. 4, no. 10, p. 246–252.
- [22] PRUDYUS, I. N., OBORZHYTSKYI, V. I. A new approach to analytical calculation of microstrip directional couplers with full structure symmetry. *Radioelectronics and Communications Systems*, 2011, vol. 54, no. 9, p. 472–480.

## About Authors ...

**Ivan PRUDYUS** was born in Ukraine in 1942. He received his M.Sc., Ph.D. and D.Sc. degree in Radioelectronics in Lviv Polytechnic Institute (Ukraine) in 1969, 1980, 2005, respectively. Since 2004 he is the head of the Institute of Telecommunications, Radioelectronics and Electronic Devices, Lviv Polytechnic National University. His research interests include antennas for communication systems, remote sensing systems.

**Valeriy OBORZHYTSKYI** was born in Ukraine, in 1949. He received the M.Sc. degree in Radioelectronics Engineering in Lviv Polytechnic Institute (Ukraine) in 1972, the Ph.D. degree in Microwave Devices and Antennas in Moscow Institute of the Electronic Techniques in 1983. His research interests are in the field of microwave network theory and methods of computer-aided design, microwave integrated multiband circuits, tunable circuits, matching circuits.